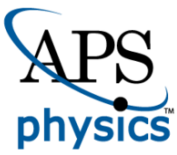

Accumulation of swimming bacteria near a solid surface

Guanglai Li, James Bensson, Liana Nisimova, Daniel Munger, Panrapee Mahautmr, Jay X. Tang, Martin R. Maxey, and Yves V. Brun

Phys. Rev. E **84**, 041932 — Published 28 October 2011

DOI: 10.1103/PhysRevE.84.041932

Accumulation of swimming bacteria near a solid surface

Guanglai Li, James Bensson, Liana Nisimova, Daniel Munger, Panrapee Mahautmr, and Jay X. Tang*

Physics Department, Brown University, Providence, RI 02912

Martin R. Maxey

Department of Applied Mathematics, Brown University, Providence, RI 02912

Yves V. Brun

Department of Biology, Indiana University, Bloomington, IN 47405

Abstract

We measured the distribution of a forward swimming strain of *Caulobacter crescentus* near a surface using a three-dimensional tracking technique based on darkfield microscopy and found that the swimming bacteria accumulate heavily within a micrometer from the surface. We attributed this accumulation to frequent collisions of the swimming cells with the surface, causing them to align parallel to the surface as they continually move forward. The extent of accumulation at the steady state is accounted for by balancing alignment caused by these collisions with the rotational Brownian motion of the micrometer-sized bacteria. We performed a simulation based on this model, which reproduced the measured results. Additional simulations demonstrated the dependence of accumulation on swimming speed and cell size, showing that longer and faster cells accumulate more near a surface than shorter and slower ones do.

* Jay_Tang@brown.edu

I. INTRODUCTION

Flagellated bacteria actively swim in water, propelled by their rotating helical flagellar filaments, which are powered by the flagellar motors [1]. A multiply flagellated bacterium such as an *E. coli* swims in more or less a straight line during a "run" and randomly changes its orientation when it "tumbles" [2]. A singly flagellated bacterium such as a *V. alginolyticus* swims back and forth by switching its swimming direction [3]. At the steady state, swimming bacteria uniformly distribute in a homogeneous bulk fluid. When there are particles carrying nutrients in the fluid, they swim towards and accumulate around the particles [4, 5], through a mechanism referred to as chemotaxis [6]. The behavior is different yet when bacteria swim near a flat solid surface. First, they tend to swim in circular trajectories rather than straight lines [3, 7, 8]. Second, they accumulate near the surface [9, 10], even without the involvement of chemotaxis. This accumulation is dictated by physical interactions, including hydrodynamic, electrostatic, and van der Waals interactions between the bacteria and the surface, as elaborated by a number of studies [7, 8, 11].

Hydrodynamic interaction has long been considered as the major contributor for the near surface accumulation of swimming bacteria. At a large distance of, say, 10 μm away from the surface, this interaction could be either attractive or repulsive, depending on whether the microswimmer propels as a "pusher" or a "puller" [9]. At close distances, the hydrodynamic interaction also depends on the length of the flagellar filament and the aspect ratio of the cell body. Excluding Brownian motion and other interactions, calculations show that the hydrodynamic interaction with the surface alone keeps a forward swimming cell moving parallel to the surface at a distance comparable to the cell body width and following a circular trajectory [12]. However, for small and fast singly-flagellated bacteria such as *V. alginolyticus* and *C. crescentus,* circular trajectories were only observed for backward swimming cells. The forward swimmers have only been observed to travel near a surface for a short period of time, and circular trajectories are rarely seen [3, 7, 10]. Therefore, we believe that hydrodynamic interaction with a solid surface is not a dominant factor for determining the forward swimming trajectories of microswimmers, especially for small and fast ones, near a surface.

In a previous report [10], we established a model that attributes the accumulation of forward swimming bacteria to the collision of the swimming cells with the surface and

the influence of rotational Brownian motion - the collision aligns the swimming direction parallel to the surface while the rotational Brownian motion randomly changes the swimming direction so that the cells have chances to swim away. This model proves successful in explaining the measured near-surface distributions for *E. coli* [9], *C. crescentus* [10], and even bull spermatozoa [13], when the swimming cells were placed between two glass surfaces 200 μm apart, and the cell density was measured in increments of 10 or 20 μm as a function of distance from the surface. A recent measurement and simulation of swimming bacterium near a surface also favor this simple model [14].

This paper extends our previous report [10], providing evidence that the model is valid even within a few micrometers from a surface. At close distances, short-range lubrication effects [15], electrostatic and van der Waals forces [11] may alter the distribution, raising concern over the model where much of these cell-surface interactions are ignored. In order to address this concern, we report new measurements of the distribution of forward swimming *C. crescentus* cells within a few micrometers from the surface using a 3-D tracking technique based on darkfield microscopy [16], which offers spatial resolution to within tenths of a micrometer. We also expand our simulation predictions to obtain results of comparable resolution. The agreement between the new measurements and simulation results demonstrates the effectiveness of the model even within short distances on the order of micrometers. Further predictions based on this model are made to show the dependence of accumulation on swimming speed and cell size.

II. OBSERVATION OF CELL DISTRIBUTION NEAR A SURFACE

A. Materials and Methods

Bacterium *C. crescentus* strain CB15 SB3860 [7] was used to examine the near-surface swimming and accumulation. Swarmer cells of this strain rarely attach to a surface due to lack of pili [17], thereby making them ideal for the study of near surface swimming. The flagellar motor of this strain rotates only in one direction and the cell swims exclusively forward. The simple behavior of this mutant simplifies the analysis of our measurements. While wild-type cells display circular trajectories when they swim backward near a surface [7], these forward swimmers do not form circular trajectories [10]. Cells of this mutant

strain were synchronized using the plate releasing method to obtain cultures with primarily swimming cells [18]. A drop of the synchronized cells was sealed between a glass slide and a coverslip with vacuum grease for optical microscopy observation. A 40× objective (Nikon Plan Apo, numerical aperture of 0.75) was used on a Nikon E800 microscope to take videos of swimming cells in darkfield mode using a CoolSnap CCD camera (Princeton Instruments) and MetaMorph software (Universal Imaging).

We applied an automated 3-D tracking microscopy technique following the method by Wu *et. al.* [16]. They showed that the image of a cell out of focus appears as a bright ring under a microscope. The ring size can be calibrated to obtain the distance of the cell from the surface. To measure the distance from a surface, we first focused the objective at the surface and then shifted the focal plane several micrometers into the glass (Fig. 1a). Although the cell body has an ellipsoidal shape (Fig. 1b), its defocused image appears as a circular ring (Fig. 1c). The distance from the surface is calibrated from the ring radius (Fig. 1d). Videos of swimming cells near the surface were taken at 20 frames per second. The thickness of the slide sample was measured by focusing on the two surfaces separately and subtracting the readings on the microscope knob with proper calibration to correct for the effects of optical refraction [19].

The image of a typical *C. crescentus* swarmer cell, shown in Fig. 1b, was acquired with a D3100 atomic force microscope (Veeco, Inc) under tapping mode. This particular cell was derived from the CB15 wildtype strain. The wild-type swarmer cells tend to attach to a glass surface. After attachment, the glass surface was rinsed with pure water and dried for convenient AFM imaging. The image was constructed using the amplitude signal of the vibrating AFM cantilever.

B. Swimming trajectories

Trajectories of forward swimming *C. crescentus* cells near the top surface of a slide sample $\sim$22 μm thick were acquired by the 3-D tracking algorithm based on images acquired through darkfield microscopy. A collection of 10 such trajectories is shown in Fig. 2. Typically, a cell collides with the surface at an angle. It then moves in close proximity while gaining alignment to swim nearly parallel to the surface in less than 1 second before it departs from the surface. These forward swimming cells do not spend a long time near the surface as

compared to backward swimming cells, which produce circular trajectories lasting up to several seconds [7].

C. Accumulation near a surface

Even though the forward swimming cells only spend a brief time near the surface, the above trajectories still give rise to a much higher chance of finding a cell at a closer distance than farther away from the surface. Over 10,000 measured $X - Z$ position data of 699 trajectories within 5 μm from the surface are plotted in Fig. 3a. There is a dense band of cells found within 1 μm from the surface. The probability density distribution is binned at 0.5 μm and the histogram of this distribution as a function of distance is shown in Fig. 3b. The count of cells in the first bin is 4.5 times that in the second one and 9.9 times that at 5 μm away. Note that the 3-D tracking method has a resolution limit of 0.2 μm in height. In practice, we set the cell with the smallest ring in a video to be at distance $Z = 0$ and relate the distances of other cells to this position. Because of this restricted choice of the zero position, no negative positions were recorded. In reality, the calculated positions of many cells yielded small positive values even if they might have made contact with the surface. This factor introduces a systematic error which would bias the results and underestimate the number of cells in the first bin of the histogram. Specifically, one notes a dense band of cells at 0.2-0.3 μm from the surface, and the band spreads beyond the first bin. The factors for this peak position offset from the zero distance include cell size variation and the fact that elongated cells can hit the surface with various orientations. In spite of the underestimate, the result clearly demonstrates that there is a strong accumulation of cells within 0.5 μm from the surface.

III. MODELING AND SIMULATION

A. Model

As shown in our previous report, the key premise of our model is that the combination of collision and rotational Brownian motion gives rise to the accumulation of microswimmers near a solid surface [10]. When a cell swims toward and then collides with a solid surface, its motion is redirected so that it becomes parallel to the surface while it continues to

move in close proximity. Excluding all other effects, the cell would cruise near the surface indefinitely, assuming constant propulsion by the rotating flagellum. In reality, a micrometer sized bacterium undergoes continuous translational and rotational Brownian motion. For a fast microswimmer, the rotational Brownian motion plays a more important role than the translational one in changing the course of its motion, by randomly altering its swimming direction. The random changes in swimming direction allow the bacterium to leave the surface. Other effects such as long range hydrodynamic interaction [9] and lubrication [15] are ignored in this model.

We discuss here specifically why much of the lubrication effect can be omitted. When a cell swims toward a surface, the lubrication effect contributes to the normal force that redirects swimming direction. We will show, however, that this process is so brief that a detailed description of lubrication effect is unnecessary in the analysis leading to steady state accumulation. We first estimate the time needed for a swimming cell to make contact with a surface. The lubrication effect increases drag for a spherical particle of radius a approaching a surface head on by a factor of $1/\varepsilon$ at a close distance of εa, where $\varepsilon < 1$ [15]. Therefore, when the cell swims toward the surface at an initial speed V_0, it slows down to $\sim \varepsilon V_0$ at the distance εa, due to the lubrication effect. The cell keeps approaching until it reaches a distance, λ, where further approach is inhibited by strong electrostatic repulsion [11] and surface roughness [20]. The distance is typically on the order of nanometers in cell medium. The time the cell takes to move from a distance a to this distance λ is $a\ln(a/\lambda)/V_0$. For *C. crescentus*, $a \sim 500$ nm and $V_0 \sim 50$ μm/s. The cell only takes ~0.06 sec to reach a position where the electrostatic repulsion [7] and solid contact [21] dominate the lubrication. This period is very short compared to the time scale considered in this paper. Therefore it is not necessary to fully describe the details of how the lubrication effect modifies the approaching process. Instead, we practically refer this process as collision, during which the lubrication effect, together with electrostatic repulsion and solid contact, provides a normal force to stop the approach and realign the cell orientation.

We also demonstrate that the lubrication torque on a sphere moving parallel to a surface has little effect on cell reorientation. Figure 4a illustrates a situation when the spherical cell body is very close to the surface. It has been shown that a spherical particle tends to roll when moving parallel to a surface, resulting from a torque caused by the lubrication effect [15]. This torque is proportional to the moving speed, $\Gamma_{lub} = -A_{lub}V$, where A_{lub}

depends on the radius of the sphere and the distance from the surface. We show that this rolling effect can be neglected by the following two estimates. Firstly, we calculate the additional rotation rate caused by this effect to the cell body and filament as a complex, which is $\Omega_{lub} = -A_{lub}V/A_{33}$. For *C. crescentus*, $A_{33} = 1.9 \times 10^{-19}$ Nms [10]. The cell body is treated as a sphere with a 0.5 μm radius. At a distance as small as 10 nm from the surface, $A_{lub} = 5.7 \times 10^{-16}$ Ns. At a typical swimming speed $V = 45$ μm/s, $\Omega_{lub} = 0.14$ rad/s, which is over an order of magnitude smaller than the typical rotation rate, $\sim$8 rad/s at $\theta = 45°$ during collision, for instance, calculated without the lubrication effect [10]. Secondly, we calculate the final angle when the cell body and filament complex stops rotating. When the bacterium stops rolling, the angle θ is determined by $\sin\theta = A_{lub}/A_{23}$. For *C. crescentus*, $A_{23} = 5.3 \times 10^{-14}$ Ns [10]. At a distance as small as 10 nm from the surface, the angle $\theta \approx 0.01$ rad, indicating that the filament only tilts up by a very small angle. In reality, the distance is usually larger than 10 nm and thus the tilt angle is even smaller. This small angle can be safely ignored when compared with rotational Brownian motion, which can cause an average change in angle of over 0.1 rad within 0.1 s.

B. Simulation

In simulation, a model bacterium (Fig 4a) is simplified and represented as a non-uniform rod (Fig. 4b) with the same hydrodynamic properties assigned as the elongated model bacterium. The length of the rod is equal to the head-to-tail length of the bacterium. The rod has a rotation center at position O, which is of a distance L_1 away from the head and L_2 away from the tail. Since the head has a larger drag per unit length than the tail does, $L_1 < L_2$, as required by the torque balance. We set $L_1 = 0.3L$ in all simulations, consistent with the known geometry of flagellated bacteria. This rod swims forward at speed V in the bulk fluid. When its head is in contact with a surface, the tail tilts toward the surface at a rotation rate Ω, which is calculated as described in our previous report [10].

The motion of the rod is dictated by swimming and Brownian motion. When the head of the rod is not in contact with the surface, the change in distance of the rotation center to the surface, y, is determined by the translational Brownian motion and the swimming direction, which is continuously altered by the rotational Brownian motion. Over a time interval Δt, $\Delta y = -V\sin\theta\Delta t + \zeta\sqrt{2D_t\Delta t}$, and $\Delta\theta = \varsigma\sqrt{2D_r\Delta t}$, where ζ and ς are random

numbers with zero mean and unit variance, D_t and D_r are the translational and rotational diffusion constant, respectively. The angle θ is positive for a cell approaching the surface and negative when swimming away. When the cell head is in contact with the surface, $\Delta y = -L_1 \Omega \Delta t \cos\theta + \zeta\sqrt{2D_t \Delta t}$, and $\Delta\theta = -\Omega\Delta t + \varsigma\sqrt{2D_r\Delta t}$. Over a typical measurement time interval of 0.05 s or longer, we note that the translational Brownian motion contributes much less than swimming to the displacement for microorganisms swimming at tens of μm/s.

When near a surface, the changes in distance and angle are also restricted by the solid surface to satisfy $y \geqslant L_1 \sin(-\theta)$ when the head is closer to the surface and $y \geqslant L_2 \sin\theta$ when the tail is closer. Similar restrictions hold when a cell is near the opposite surface. Knowing D_t and D_r, we can track the distance y and angle θ over time. The distance of the head from the surface h, which is what was measured in the experiment, is determined by $h = y + L_1 \sin\theta$. In the simulation, we place a swimming bacterium between two surfaces and record the distance from the bottom surface over time. The probability distribution of a cell at distance h is obtained by tracking a cell swimming between the two surfaces over 10^5 - 10^7 seconds, depending on the thickness of the fluid between the two surfaces, to ensure sufficient sampling of the distances for a statistically reliable histogram.

C. Distribution of cell density near a surface

When confined between two surfaces, a swimming bacterium travels between the two surfaces repeatedly. Fig. 5 shows examples of the distance over time for a *C. crescentus* swimming between two surfaces separated by 200 μm and 20 μm, respectively. The cell swims at 45 μm/s and has a rotational diffusion constant of 0.1 rad^2/s. Other typical parameters for *C. crescentus* are $D_t = 0.1$ μm^2/s, $L = 6$ μm, and $L_1 = 1.8$ μm. In both cases, the model cells swim randomly up and down between the two surfaces. They stay near a surface temporarily before moving off into the bulk, consistent with experimental observations (Fig. 2). They can either go to the other surface or turn back to the surface they left from, dictated randomly by the rotational Brownian motion. Fourier energy spectrum performed for the entire simulated time series is continuous and has no defined peaks (data not shown), confirming that the simulated process is random and has no periodic pattern.

It is evident from the simulated trajectories that the cells spend more time near a surface, as shown in Fig. 5. A histogram of the probability density, ρ, of a cell staying at a distance

from a surface, using the bin size of 10 μm, is shown in Fig. 6a for two surfaces separated by 200 μm. There is a strong accumulation near either surface. The probability density decreases quickly with the distance. The first bar near a surface is about 4 times as high as the second one, and nearly 7 times as that in the middle between the two surfaces. The level of accumulation strongly depends on the bin size. If we reduce the bin size to 0.5 μm, we see a 9 times higher density of cells in the first bar than that when the bin size is as large as 10 μm (Fig. 6b). The first bar is 6 times as high as the second one, which does not differ significantly from the ratio in the case of the 10 μm bin size. There is a similarity between the density distribution profile of these two bin sizes if only the first few bars are compared. The height of the bars in the middle has little dependence on the bin size.

Similar results are obtained for two surfaces separated by 20 μm. Binned at 2 μm, the first bar is 5 times as high as the second one and about 8 times as the one in the middle (Fig. 7a). When the bin size is reduced to 0.5 μm (Fig. 7b), the first bar is 3 times as high as that when the bin size is 2 μm. Since the density depends on the bin size, it is important to specify the bin size that is commensurate with experiments when studying accumulation near a surface.

Evidence for the simulated distribution is provided by the experimental measurement. A comparison between simulated (open symbols) and measured (closed symbols) probability density is shown in Fig. 3c for *C. crescentus* swimming between two surfaces separated by 22 μm. To convert the count in the measurement into probability density, Fig. 3b was rescaled so that the total probability within 5 μm from the surface is the same as the simulated in the same range. The simulated distribution agrees with the measurement well.

D. Accumulation factor as a function of swimming speed, cell length, and sample thickness

In the following discussion, we introduce a parameter called the accumulation factor to compare the extent of near surface accumulation as a function of swimming speed, the rotational diffusion constant, and the sample thickness. The accumulation factor is defined as the ratio of the probability density at the first bar near a surface to the average probability density over all distances, namely, ρ_s/ρ_0. The actual value of this factor depends on the choice of bin thickness. For consistent comparison, we choose the bin size of 0.5 μm, which

has more biological relevance than a much larger thickness such as 10 μm. Considering the length of pili and surface polymers responsible for adhesion, a bacterium has a large chance to adhere to a surface when it is within 1 μm or so from the surface.

In the simulation system where swimming bacteria are placed between two surfaces, the accumulation factor depends on the swimming speed, the rotational diffusion constant dictated by the head-to-tail length of the cell, and the sample thickness, i.e., the separation between the two surfaces. The accumulation factor always increases with the sample thickness, as more bacteria are available to accumulate near the boundary surface in a thicker sample (Fig. 8). The accumulation factor increases faster with thickness when the sample is thinner. It reaches a plateau when the sample is sufficiently thick.

In thicker samples, the accumulation factor increases with swimming speed (Fig. 8a), as faster swimming cells far away from the surface can contribute more to near surface accumulation than slower ones. When the sample is very thin, however, our simulation shows that slower swimming cells accumulate slightly more near the surface (inset in Fig. 8a). This property can also be explained by analyzing the physics of the process. In a thin sample, all the cells are close to the surfaces and faster swimming speed is not required to transport more cells to the surface. At the same rotational diffusion constant, thus the same cell size, a faster swimming cell rotates faster towards the direction parallel to the surface after collision. This rapid rotation actually reduces the accumulation by reducing the time spent close to the surface. Therefore, we expect the faster swimming cells to accumulate less near a surface in a thinner sample.

At a fixed swimming speed, the accumulation level decreases with an increasing rotational diffusion constant (Fig. 8b). Two effects contribute to this property. First, longer cells with a smaller rotational diffusion constant have more persistent swimming trajectories; therefore, from the same distance away they tend to reach the surface more easily and contribute more to the accumulation than shorter swimmers, which change directions more quickly. Second, because cells with smaller rotational diffusion constants are longer, at the same swimming speed, they tend to spend more time gliding on the surface after collision, thereby enhancing the level of accumulation.

E. Maximum accumulation factor as a function of swimming speed and rotational diffusion constant

One interesting question to ask is: what is the maximum extent of accumulation near a surface? In natural environments, a surface usually submerges in bulk water. Swimming cells at any distance could contribute to near surface accumulation. This situation is equivalent to the accumulation when the sample is infinitely thick. In the simulation, we increase the sample thickness until there is no discernible change in accumulation level, typically after 1 to 3 mm depending on the swimming speed and the rotational diffusion constant. This accumulation factor is taken as the maximum accumulation. The simulation results (Fig. 9) preserve the essential features that faster swimmers with smaller rotational diffusion constants accumulate more near a surface submerged in an infinitely large body of water.

If there is a mixed population of bacteria swimming at the same speed, larger cells will accumulate more near the surface. The rotational diffusion constant is inversely proportional to L^3 for a rod. In Fig. 9, $D_r = 0.1$ rad^2/s is for typical *C. crescentus*, which has a head-to-tail length of about 6 μm. A cell with $D_r = 0.5$ rad^2/s would correspond to a head-to-tail length of 3.5 μm, while $D_r = 0.02$ rad^2/s corresponds to a head-to-tail length of 10.3 μm. The simulation shows that cell length has a larger influence on accumulation than swimming speed. This is not surprising given the dependence of D_r on cell length to the third power.

IV. CONCLUDING REMARKS

This study increases spatial resolution by an order of magnitude with more clearly defined near-surface layers and associated dynamics than previous studies [9, 10]. We have measured the cell density distribution of forward swimming cells of *C. crescentus* near a surface with 3-D tracking dark field microscopy and found that these cells strongly accumulate within 1 μm from a surface. We elaborate on a collision based model that quantitatively accounts for the accumulation by analysis of cell collision with the surface and rotational Brownian motion of the microswimmers. Besides reproducing the observed density distribution, our simulation also shows that the accumulation level depends on both the swimming speed and the rotational diffusion constant, which is determined by cell size. Larger and faster swimming bacteria tend to accumulate more near a surface.

Accumulation of microswimmers within a few micrometers from a surface is highly relevant to bacterial adhesion and biofilm formation. The most important events in bacterial adhesion tend to occur when the cell body reaches within an order of 1 μm so that adhesive cell appendages such as pili [22, 23] and surface polymers [24] can make contact with the surface. The closer a bacterium to a surface, the larger the chance for it to adhere. Our result shows a strong tendency of accumulation of microswimmers at close distances, which is consistent with previous observations that swimming greatly enhances bacterial adhesion and biofilm formation in comparison with their nonmotile mutants or counterparts [17, 22, 25].

The strong accumulation near a surface offers a convenient system for the study of collective behavior of swimming bacteria [26]. Our measurements and analysis are performed for dilute bacterial suspensions, where the cell-cell interaction is ignored. As shown in the simulation, however, the maximum accumulation within 0.5 μm from a surface for a real bacterium *C. crescentus* can be more than 50 times that of the average density. This may well divide a bacterial suspension into two regimes - in the bulk where it is in the dilute limit; and near the surface where the cell density may be concentrated enough for the collective behavior to emerge, for which there have been interesting theoretical and simulation work [27, 28].

Note that we are only dealing with singly flagellated forward swimming bacteria, which do not follow circular trajectories near a surface. Singly flagellated backward swimming cells follow circular trajectories near a surface and stay near the surface for much longer times [7]. Therefore, backward swimming cells are expected to accumulate near a surface more strongly than forward swimming cells. The additional long dwell time of backward swimming cells could depend on a number of factors, such as the structure and flexibility of the flagellar filament and/or hook, the geometric shape of the cell body, and attractive hydrodynamic force towards the surface. The exact mechanism leading to this difference in forward and backward swimming cells is not yet understood. Nevertheless, our results clearly demonstrate the significant roles of cell-surface collision and rotational Brownian motion in bacterial near surface swimming.

We acknowledge support of this work by NIH GM077648, NSF DUE 0734234 and NSF PHY 1058375. We thank Professors B. Ely for kindly providing us the forward swimming

bacterial strains.

[1] H. C. Berg, *E. coli in motion* (Springer, New York, 2004).

[2] H. C. Berg and D. A. Brown, Nature **239**, 500 (1972).

[3] S. Kudo, N. Imai, M. Nishitoba, S. Sugiyama, and Y. Magariyama, FEMS Microbiol. Lett. **242**, 221 (2005).

[4] G. A. Jackson, Limnol. Oceanogr. **34**, 514 (1989).

[5] T. Fenchel, Science **296**, 1068 (2002).

[6] M. Eisenbach, J. W. Lengeler, M. Varon, D. Gutnick, R. Meili, R. A. Firtel, J. E. Segall, G. M. Omann, A. Tamada, and F. Murakami, *Chemotaxis* (Imperical College Press, London, 2004).

[7] G. Li, L.-K. Tam, and J. X. Tang, Proc. Nat. Acad. Sci. **105**, 18355 (2008).

[8] P. D. Frymier, R. M. Ford, H. C. Berg, and P. T. Cummings, Proc. Nat. Acad. Sci. USA **92**, 6195 (1995).

[9] A. P. Berke, L. Turner, H. C. Berg, and E. Lauga, Phys. Rev. Lett. **101**, 038102 (2008).

[10] G. L. Li and J. X. Tang, Phys. Rev. Lett. **103**, (2009).

[11] M. A. Vigeant and R. M. Ford, Appl. Environ. Microbiol. **63**, 3474 (1997).

[12] H. Shum, E. A. Gaffney, and D. J. Smith, Proc. R. Soc. A - Math. Phys. Eng. Sci. **466**, 1725 (2010).

[13] L. Rothschild, Nature **198**, 1221 (1963).

[14] K. Drescher, J. Dunkel, L. H. Cisneros, S. Ganguly, and R. E. Goldstein, Proc. Nat. Acad. Sci. USA **108**, 10940 (2011).

[15] E. Lauga, W. R. DiLuzio, G. M. Whitesides, and H. A. Stone, Biophys. J. **90**, 400 (2006).

[16] M. M. Wu, J. W. Roberts, and M. Buckley, Exp. Fluids **38**, 461 (2005).

[17] D. Bodenmiller, E. Toh, and Y. V. Brun, J. Bacteriol. **186**, 1438 (2004).

[18] S. T. Degnen and A. Newton, J. Mol. Biol. **129**, 671 (1972).

[19] G. Li and J. Tang, Phys. Rev. E **69**, 061921 (2004).

[20] J. R. Smart and D. T. Leighton, Phys. Fluids A **1**, 52 (1989).

[21] R. H. Davis, Y. Zhao, K. P. Galvin, and H. J. Wilson, Phil. Trans. R. Soc. Lond. A (2003) 361, 871-894 **361**, 871 (2003).

[22] L. A. Pratt and R. Kolter, Mol. Microbiol. **30**, 285 (1998).

[23] E. Bullitt and L. Makowski, Biophy. J. **74**, 623 (1998).

[24] H. Morisaki, S. Nagai, H. Ohshima, E. Ikemoto, and K. Kogure, Microbiology **145**, 2797 (1999).

[25] J. Dunne, W. Michael, Clin. Microbiol. Rev. **15**, 155 (2002).

[26] M. Wu, J. W. Roberts, S. Kim, D. L. Koch, and M. P. DeLisa, Appl. Environ. Microbiol. **72**, 4987 (2006).

[27] J. P. Hernandez-Ortiz, C. G. Stoltz, and M. D. Graham, Phys. Rev. Lett. **95**, 204501 (2005).

[28] D. Saintillan and M. J. Shelley, Phys. Rev. Lett. **100**, 046311 (2008).

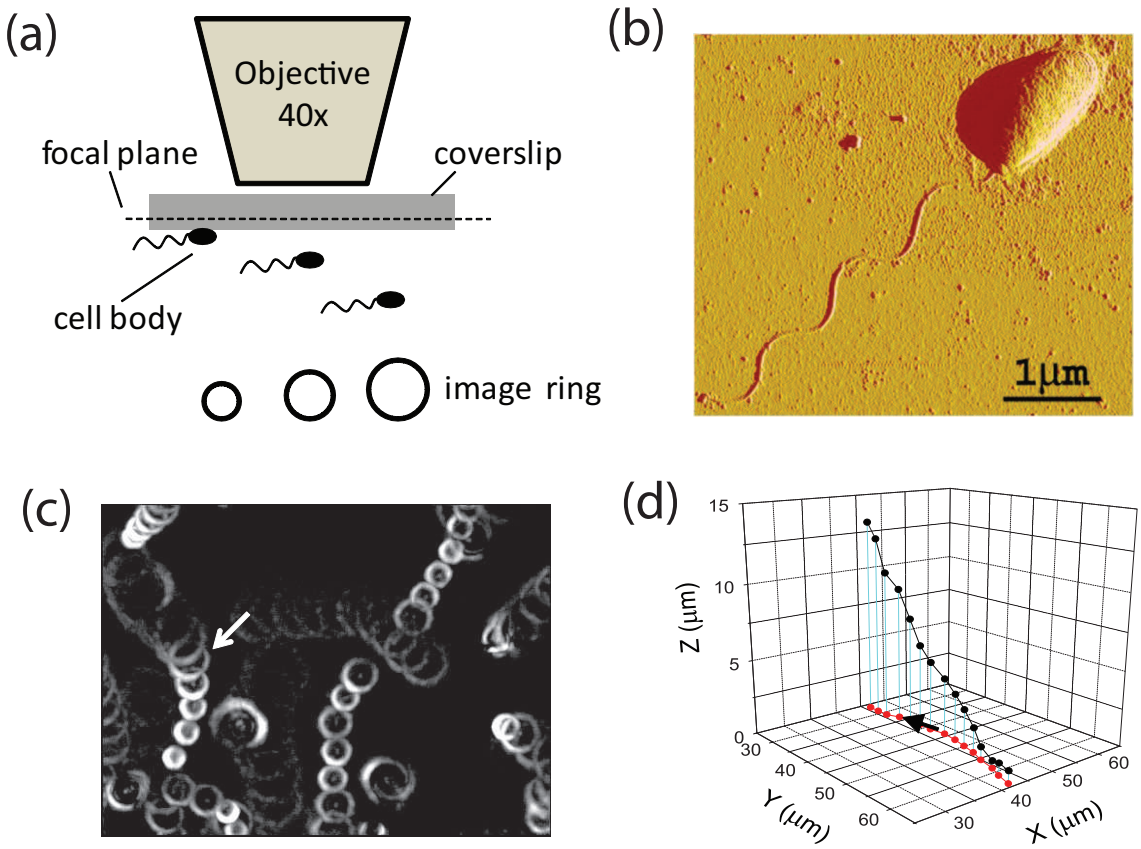

Figure 1. (color online) (a) Schematic drawing of the setup. The focal plane is set at a few micrometers within the coverslip so that the ring size varies monotonically with the distance of the cell body from the coverslip surface. (b) Atomic force microscopy image of a *C. crescentus* CB 15 wildtype swarmer cell dried on a glass coverslip. (c) An overlay of images of swimming cells. The video was taken at 20 frames per second. Only one of every five frames was kept in the overlay to better illustrate the trajectories as sets of discrete rings. (d) Three dimensional trajectories (black) and their projection on the $X-Y$ surface (red or gray) of the cell marked by a white arrow in (c). The arrow in (d) indicates the swimming direction.

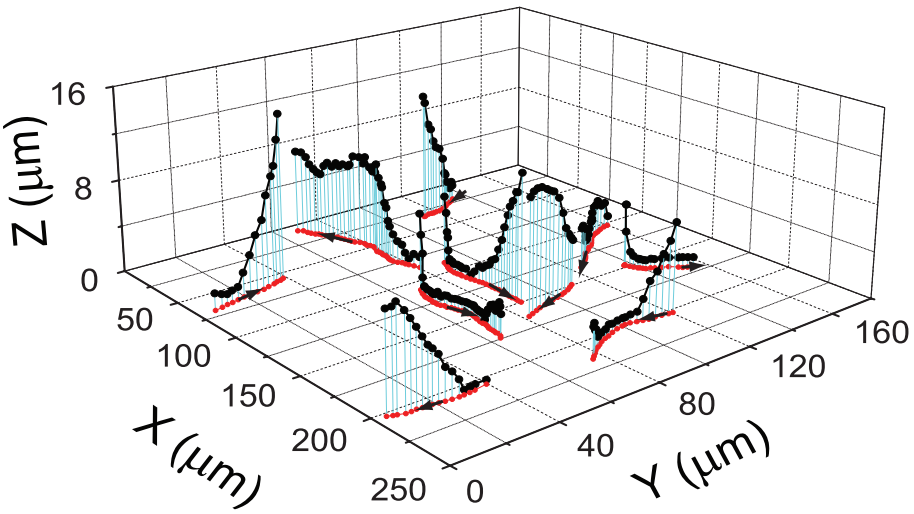

Figure 2. (color online) A collection of 3-D trajectories (black) and their projections on the $X-Y$ surface (red or gray). Arrows on the projections indicate the swimming directions.

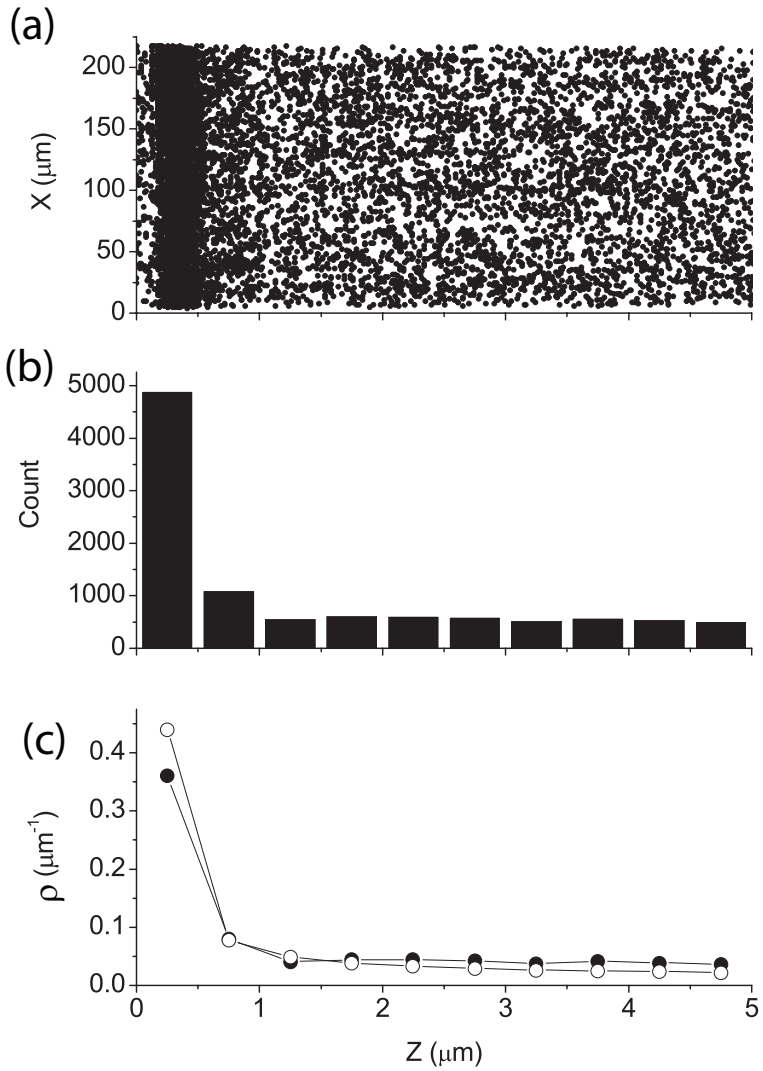

Figure 3. (a) $Z-X$ plot of over 10,000 measured positions from 699 cell trajectories to visualize near surface distribution. (b) Histogram of the distance of 0.5 μm bin size. (c) A comparison between the measured (closed circle) and simulated (open circle) probability density (ρ) distributions.

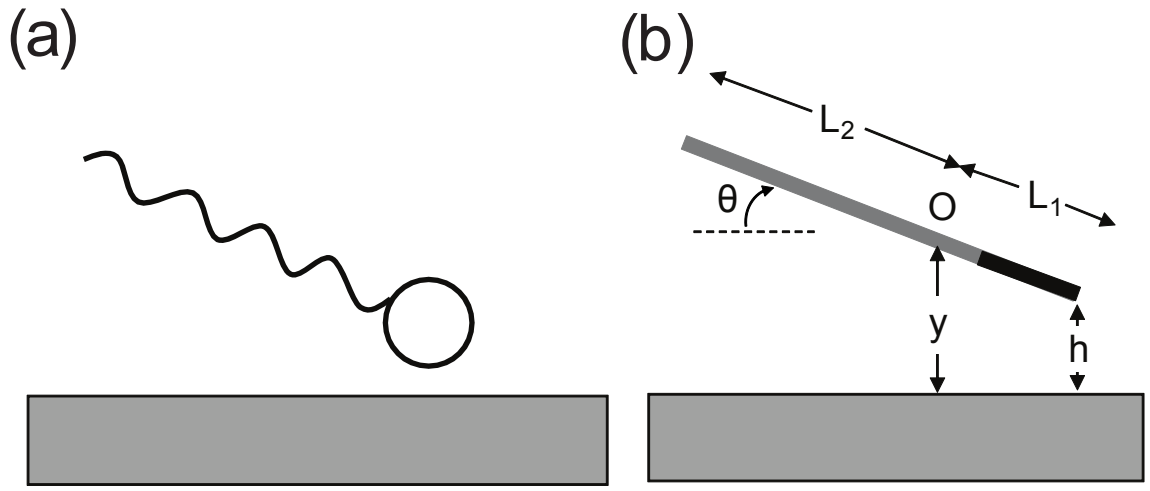

Figure 4. (a) A model bacterium swimming near a surface, which has a cell body and a rigid flagellar filament. (b) Further simplified rod model representing the model bacterium swimming near a surface. Here the body of the bacterium is depicted by the short black segment, and the flagellum by the long gray segment.

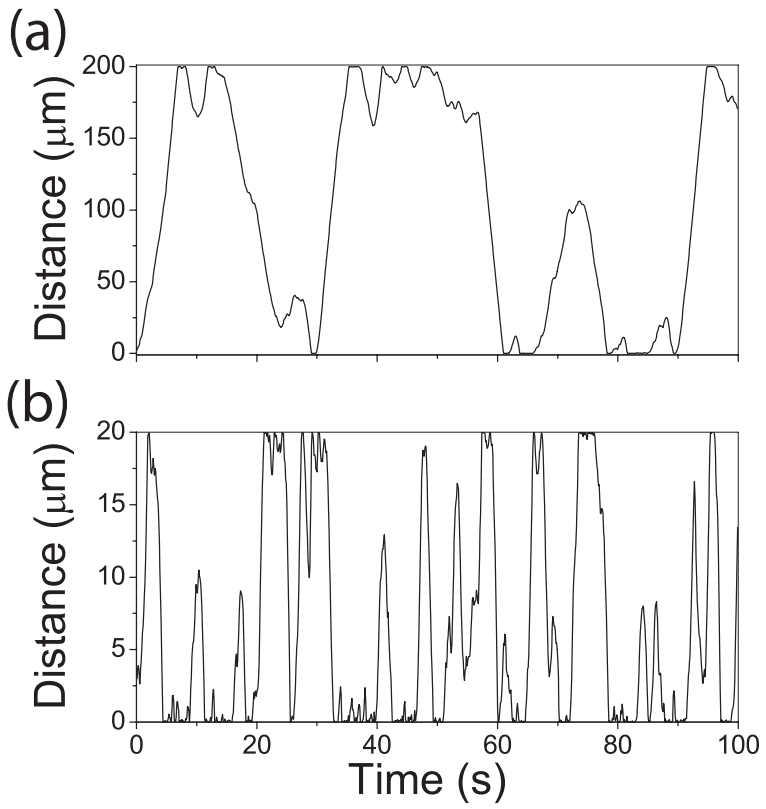

Figure 5. Examples of the distance of a swimming *C. crescentus* cell in a 200 μm thick channel (a) and a 20 μm thick channel (b), each as a function of time, simulated with a swimming speed of 45 μm/s and a rotational diffusion constant of 0.1 rad^2/s.

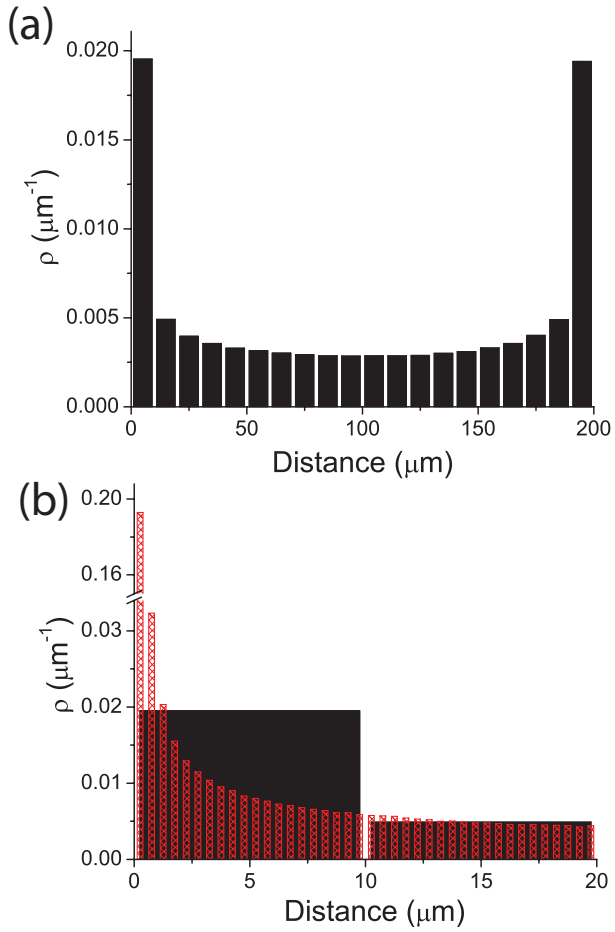

Figure 6. (color online) Simulated probability density (ρ) distribution of *C. crescentus* as a function of distance from a surface in a 200 μm thick channel. (a) Whole range distribution shown with a bin size of 10 μm; (b) A comparison of distributions between bin size 10 (black) and 0.5 (red hatched) μm within the first 20 μm from the surface.

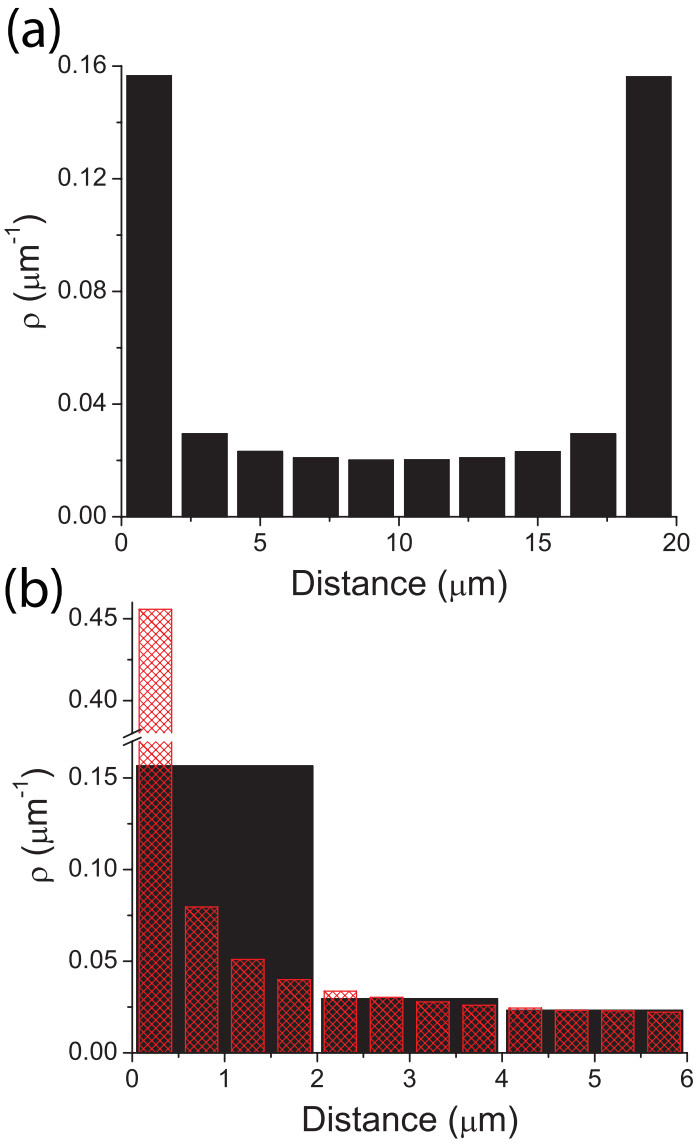

Figure 7. (color online) Simulated probability density (ρ) distribution of *C. crescentus* as a function of distance from a surface in a 20 μm thick channel. (a) Whole range distribution shown with a bin size of 2 μm; (b) Comparison of distributions between bin size 2 (black solid) and 0.5 (red hatched) μm within the first 6 μm from the surface.

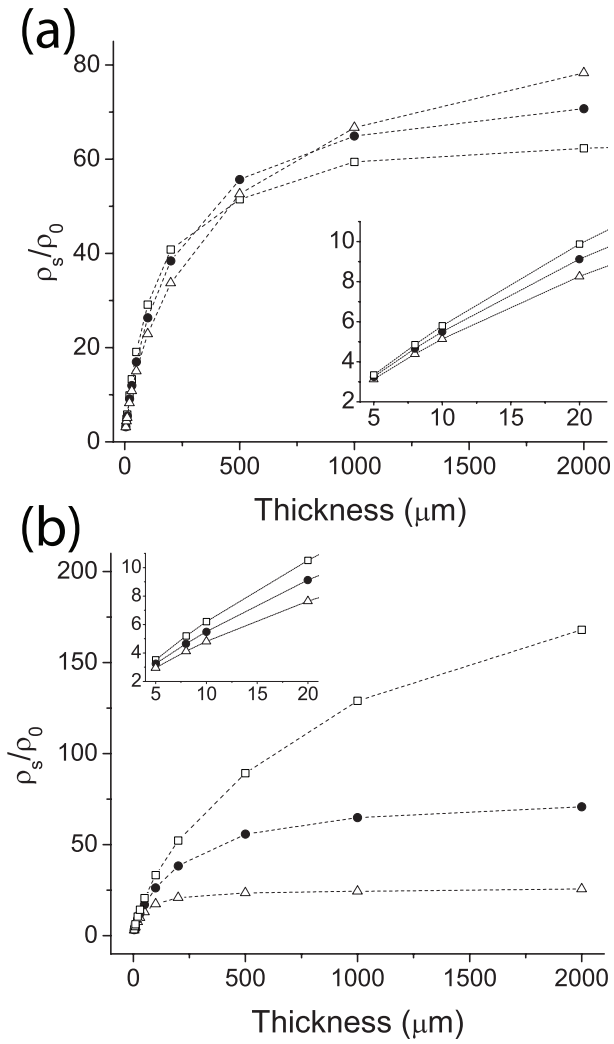

Figure 8. (a) Dependence of the accumulation factor, i.e., the ratio of the surface density ρ_s to the average density ρ_0, as a function of sample thickness for cells swimming at 20 (square), 45 (circle), and 100 (triangle) μm/s. Inset shows the details within 20 μm from the surface. D_r=0.1 rad^2/s^{-1}. (b) Dependence of the accumulation factor as a function of sample thickness for cells with rotational diffusion constants of 0.02 (square), 0.1 (circle), and 0.5 (triangle) rad^2/s^{-1}. The swimming speed is fixed at 45 μm/s. Inset shows the details within 20 μm from the surface.

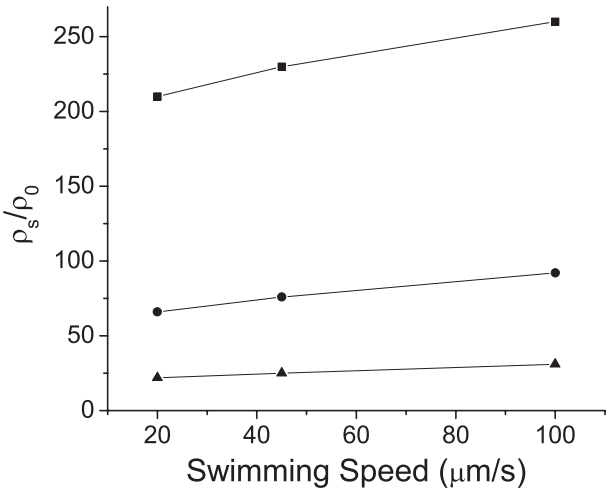

Figure 9. Maximum accumulation factor as functions of swimming speed with rotational diffusion constants of 0.02 (square), 0.1 (circle), and 0.5 (triangle) $\mathrm{rad}^2/\mathrm{s}$.